Advances in Difference Equations
a SpringerOpen Journal

RESEARCH Open Access

Analysis of an improved fractional-order model of boundary formation in the *Drosophila* large intestine dependent on Delta-Notch pathway

Deshun Sun[1,2*†], Lingyun Lu[3†], Fei Liu[4], Li Duan[1], Daping Wang[1] and Jianyi Xiong[1*]

*Correspondence:
Sun_deshun@hit.edu.cn;
jianyixiong@126.com
[1]Shenzhen Key Laboratory of Tissue Engineering, Shenzhen Laboratory of Digital Orthopedic Engineering, Shenzhen Second People's Hospital, The First Hospital Affiliated to Shenzhen University, Health Science Center, Shenzhen 518035, P.R. China
[2]Shenzhen Institute of Advanced Technology, Chinese Academy of Sciences, Shenzhen 518035, P.R. China
Full list of author information is available at the end of the article
†Equal contributors

Abstract

In this paper, an improved fractional-order model of boundary formation in the *Drosophila* large intestine dependent on Delta-Notch pathway is proposed for the first time. The uniqueness, nonnegativity, and boundedness of solutions are studied. In a two cells model, there are two equilibriums (no-expression of Delta and normal expression of Delta). Local asymptotic stability is proved for both cases. Stability analysis shows that the orders of the fractional-order differential equation model can significantly affect the equilibriums in the two cells model. Numerical simulations are presented to illustrate the conclusions. Next, the sensitivity of model parameters is calculated, and the calculation results show that different parameters have different sensitivities. The most and least sensitive parameters in the two cells model and the 60 cells model are verified by numerical simulations. What is more, we compare the fractional-order model with the integer-order model by simulations, and the results show that the orders can significantly affect the dynamic and the phenotypes.

Keywords: Delta-Notch signaling pathway; Fractional-order differential equations; Local stability analysis; Sensitive analysis

1 Introduction

The *Drosophila* large intestine occupies a major middle portion of the hindgut and is subdivided into dorsal and ventral domains with distinct cell types, and a one-cell-wide strand of boundary cells is induced between them for wild-type embryos. Takashima et al. [1] reported that the identity and localization of boundary cells are mainly determined by Delta, Notch, and activated Notch genes.

For such developmental patterning problems, computational approaches are breaking new ground in understanding how embryos form. Different kinds of computational strategies [2, 3] have been proposed. For example, in 2002, Matsuno et al. [4] analyzed the mechanism of Notch-dependent boundary formation in the *Drosophila* large intestine by genomic object net (GON). Besides, ordinary differential equation (ODE), partial differential equation (PDE), and colored Petri nets are also employed to describe the developmental

Springer

patterning [5]. The research of the boundary formation in the *Drosophila* large intestine in vivo has been widely explored, but the research in computing is scarce.

Fractional-order systems have been applied in biological systems to better understand the complex behavioral patterns [6–15]. The fractional-order differential equation provided a powerful tool for characterizing memory and hereditary properties of the systems when compared to the integer-order models, and these effects cannot be neglected. For instance, Carla et al. [15] proposed a fractional-order differential equation model to analyze the clinical implications of diabetes mellitus in the dynamics of tuberculosis transmission and proved the stability of disease-free and endemic equilibriums based on the reproduction number. Almeida et al. [11] described the dynamic of SEIR-type epidemics with treatment policies by the fractional-order differential equations. The local asymptotic stability of two equilibriums was proved and the numerical simulations were presented to illustrate the conclusions. In addition, the memory property of the fractional-order differential equation allows the integration of more information from the past, which translates in more accurate predictions for the model. For example, in 2012, Diethelm et al. [8] proposed a fractional-order differential equation model for the simulation of the dynamics of a dengue fever outbreak. By simulations, the author proved that the nonlinear fractional order differential equation model can more accurately simulate the dynamics of infectious diseases than the classical ordinary differential equations. In 2013, Gilberto et al. [9] proposed a nonlinear fractional order model to explore the outbreaks of influenza A(H1N1), and the results showed that the epidemic peak of SEIR fractional epidemic model is more consistent with the peak of the real epidemic data and the mean square error is lower than in the classical model. What is more, in 2020, Lu et al. [16] proposed a fractional-order SEIHDR system to analyze the dynamic behavior of COVID-19. Similarly, the results showed that the fractional-order model also has a better fitting of the data on Beijing, Shanghai, Wuhan, Huanggang, and other cities when compared with the integer-order system. Because of the above-mentioned research, we found that the fractional-order equations may have more potential in application on a real-life system.

With the aforementioned ideas in mind, the Notch signaling pathway is highly conserved in evolution and has significant hereditary properties. Fractional-order differential equation seems much suited for modelling the Notch signal pathway. Therefore, fractional-order differential equations were used to model the mechanism of Notch-dependent boundary formation in the *Drosophila* large intestine.

The purpose of this paper is to analyze the local asymptotic stability of two equilibriums, interpret the experimental results of the boundary cell patterning in the large intestine published in [1, 17, 18] (see Fig. 1), and get the following scenarios (Fig. 1(a)–1(c)) by adjusting sensitive parameters in our model.

2 The improved mathematical model

In 2017, our previous work [18] proposed the following model:

$$\begin{cases} \frac{dD_i}{dt} = \frac{\lambda}{1+\Delta\cdot A_i} - d_1 D_i - \sum_{NG(i)} f_1 \cdot D_i, \quad 1 \le i \le NC, \\ \frac{dN_i}{dt} = \lambda_N - d_2 N_i + \sum_{j\in NG(i)} f_2 \cdot D_j - \frac{aN_i}{bD_i+N_i}, \\ \frac{dA_i}{dt} = -d_3 A_i + \frac{aN_i}{bD_i+N_i}, \end{cases} \tag{1}$$

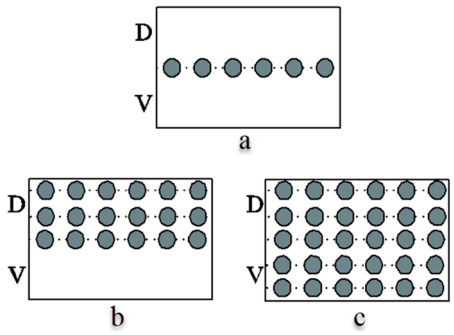

Figure 1 The experimental result of the boundary formation in the *Drosophila* large intestine published in [1, 17, 18]. (**a**) The phenotype of wild type; (**b**) to (**c**) The phenotype of over-expression of Notch. Each filled circle represents a boundary cell. *D* and *V* denote the dorsal and ventral domains, respectively

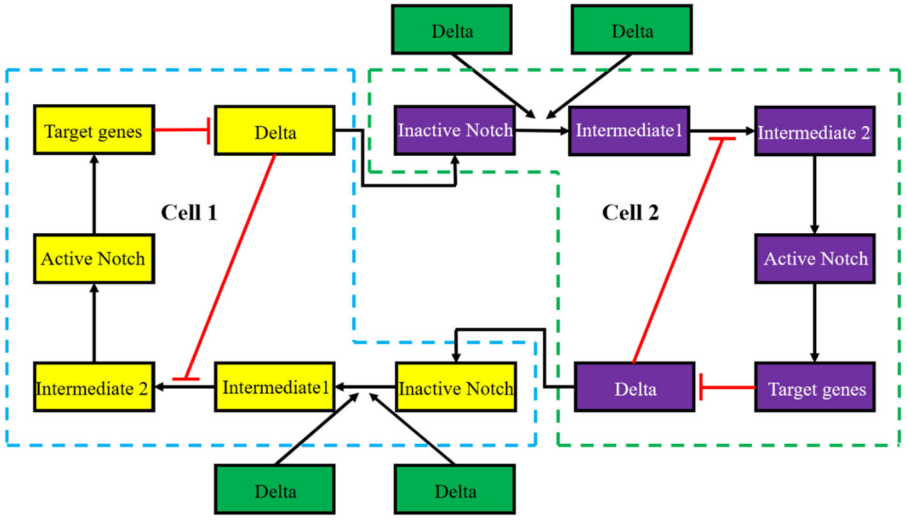

Figure 2 The mechanism of Delta-Notch signaling pathway in two cells

where D_i, N_i, and A_i represent the concentration of Delta proteins, inactive, and active Notch proteins in ith cell, respectively. λ is the production of Delta, and Δ is the inhibition coefficient caused by activated Notch. This is because activated Notch can inhibit the production of Delta in the same cell. d_i, $i = 1, 2, 3$, means the degradation rate of Delta, inactive and activated Notch. f_1 denotes the binding rate between the Delta and the neighboring Notch in ith cell. Similarly, f_2 denotes the binding rate between the Notch and the neighboring Delta in ith cell. λ_N denotes the production rate of inactive Notch. a represents the transformation rate of Notch proteins from the inactive state to the active state, while b describes the inhibition effect of Delta on Notch.

However, Notch signaling pathway is highly conserved in evolution, and the fractional-order differential equation can powerfully characterize memory and hereditary properties of systems when compared to integer-order models. Therefore, the fractional differential equations are employed to model the Notch signal pathway in this paper.

According to the mechanism of Delta-Notch signaling pathway in two cells (Fig. 2), when a Delta ligand binds to the neighboring Notch in ith cell, the binding rate is related to the concentration of the Notch receptor; therefore, we use $\sum_{j\in NG(i)} f_1 D_i N_j$ instead of the former $\sum_{j\in NG(i)} f_1 D_i$. Similarly, we change $\sum_{j\in NG(i)} f_1 N_i$ into $\sum_{j\in NG(i)} f_1 D_j N_i$. What is more, if the production rate of active Notch is $\frac{aN_i}{bD_i+N_i}$, and when the expression of Delta is 0, the

concentration of active Notch is $\frac{a}{d_3}$ in two cells. This is a contradiction. Because if there is no Delta ligand, the concentration of active Notch will be 0 in biological knowledge. Therefore, compared to $\frac{aN_i}{bD_i+N_i}$, $\frac{a(\sum_{j\in NG(i)} D_jN_i)}{b+(\sum_{j\in NG(i)} D_jN_i)}$ is more appropriate.

Thus, an improved model based on fractional-order differential equations was proposed as follows:

$$\begin{cases} \frac{d^\alpha D_i}{dt} = \frac{\lambda^\alpha}{1+\Delta^\alpha A_i} - \sum_{j\in NG(i)} f_1^\alpha D_iN_j - d^\alpha D_i, \quad 1 \le i \le NC, \\ \frac{d^\alpha N_i}{dt} = \lambda_N^\alpha + \sum_{j\in NG(i)} f_1^\alpha D_jN_i - d^\alpha N_i, \\ \frac{d^\alpha A_i}{dt} = \frac{a^\alpha(\sum_{j\in NG(i)} D_jN_i)}{b^\alpha+(\sum_{j\in NG(i)} D_jN_i)} - d^\alpha A_i, \end{cases} \tag{2}$$

where α $(0 < \alpha \le 1)$ is the order of the fractional derivative. $\frac{d^\alpha D_i}{dt}$, $\frac{d^\alpha N_i}{dt}$, and $\frac{d^\alpha A_i}{dt}$ denote the Caputo fractional derivative. For example, the Caputo fractional derivative of $\frac{d^\alpha D_i}{dt}$ is defined as follows:

$$\frac{d^\alpha D_i}{dt} = I^{n-\alpha}\frac{d^n D_i}{dt^n} = \frac{1}{\Gamma(n-\alpha)}\int_0^t (t-s)^{(n-\alpha-1)} D_i^{(n)}(s)\,ds, \tag{3}$$

where $n-1 < \alpha < n$, $n \in \mathbb{N}$ and $\Gamma(\bullet)$ is the gamma function. When $0 < \alpha < 1$,

$$\frac{d^\alpha D_i}{dt} = \frac{1}{\Gamma(1-\alpha)}\int_0^t \frac{D_i'(s)}{(t-s)^\alpha}\,ds. \tag{4}$$

Biologically speaking, $\frac{d^\alpha D_i}{dt}$, $\frac{d^\alpha N_i}{dt}$, and $\frac{d^\alpha A_i}{dt}$ represent the change rate of the concentration of Delta proteins, inactive and active Notch proteins with hereditary properties.

3 Well-posedness

In the following, the well-posedness (uniqueness, nonnegativity, and boundedness of solutions) of two cells is studied.

The model of system (2) has NC cells with $3 \times NC$ differential equations. As a result, it is impossible to analyze such a big system in theory. However, we can analyze two cells in theory and map into high dimensional equations. Therefore, the dynamic characteristic of two cells is explored.

Firstly, based on system (2), the model of two cells is proposed according to Fig. 2:

$$\begin{cases} \frac{d^\alpha D_1}{dt} = \frac{\lambda^\alpha}{1+\theta^\alpha A_1} - f^\alpha D_1N_2 - d^\alpha D_1, \\ \frac{d^\alpha N_1}{dt} = \lambda_N^\alpha + f^\alpha D_2N_1 - d^\alpha N_1, \\ \frac{d^\alpha A_1}{dt} = \frac{a^\alpha D_2N_1}{b^\alpha+D_2N_1} - d^\alpha A_1, \\ \frac{d^\alpha D_2}{dt} = \frac{\lambda^\alpha}{1+\theta^\alpha A_2} - f^\alpha D_2N_1 - d^\alpha D_2, \\ \frac{d^\alpha N_2}{dt} = \lambda_N^\alpha + f^\alpha D_1N_2 - d^\alpha N_2, \\ \frac{d^\alpha A_2}{dt} = \frac{a^\alpha D_1N_2}{b^\alpha+D_1N_2} - d^\alpha A_2. \end{cases} \tag{5}$$

3.1 Nonnegativity and boundedness

Firstly, we prove that $D_1(t) \ge 0$, $\forall t \ge 0$, assuming $D_1(0) > 0$ for $t = 0$. Let us suppose that $D_1(t) \ge 0$, $\forall t \ge 0$ is not true. Thus, there exists $t_1 > 0$ such that $D_1(t) > 0$ for $0 \le t < t_1$, $D_1(t_1) = 0$, and $D_1(t) < 0$ for $t > t_1$.

From the first equation of (5), we have $\frac{d^\alpha D_1(t)}{dt}|_{t=t_1} > 0$. Based on Corollary 1 of [19], we get $D_1(t_1^+) > 0$, which contradicts the fact $D_1(t_1^+) < 0$. Therefore, we have $D_1(t) \geq 0$, $\forall t \geq 0$. Using the same arguments, $N_1(t) \geq 0$, $A_1(t) \geq 0$, $D_2(t) \geq 0$, $N_2(t) \geq 0$, $A_2(t) \geq 0$, $\forall t \geq 0$. Next, we will prove the boundedness.

We define a function $w(t) = D_1(t) + N_1(t) + A_1(t) + D_2(t) + N_2(t) + A_2(t)$. From equation (5), we obtain

$$\begin{aligned}
&\frac{d^\alpha w(t)}{dt} + \delta w(t) \\
&= \frac{\lambda^\alpha}{1+\theta^\alpha A_1} - f^\alpha D_1 N_2 - d^\alpha D_1 + \lambda_N^\alpha + f^\alpha D_2 N_1 - d^\alpha N_1 + \frac{a^\alpha D_2 N_1}{b^\alpha + D_2 N_1} \\
&\quad - d^\alpha A_1 + \frac{\lambda^\alpha}{1+\theta^\alpha A_2} - f^\alpha D_2 N_1 - d^\alpha D_2 + \lambda_N^\alpha + f^\alpha D_1 N_2 - d^\alpha N_2 + \frac{a^\alpha D_1 N_2}{b^\alpha + D_1 N_2} \\
&\quad - d^\alpha A_2 + \delta D_1(t) + \delta N_1(t) + \delta A_1(t) + \delta D_2(t) + \delta N_2(t) + \delta A_2(t) \\
&\leq 2\lambda^\alpha + 2\lambda_N^\alpha + 2a^\alpha + \big(\delta - d^\alpha\big)\big(D_1(t) + N_1(t) + A_1(t) + D_2(t) + N_2(t) + A_2(t)\big).
\end{aligned}$$

Taking $\delta = d^\alpha$, $\frac{d^\alpha w(t)}{dt} + \delta w(t) \leq 2\lambda^\alpha + 2\lambda_N^\alpha + 2a^\alpha$. Based on [20], the boundedness is proved.

3.2 Existence and uniqueness

Consider a mapping $F(X) = (F_1(X), F_2(X), F_3(X), F_4(X), F_5(X), F_6(X))$, where

$$X = \begin{bmatrix} D_1 \\ N_1 \\ A_1 \\ D_2 \\ N_2 \\ A_2 \end{bmatrix}, \qquad \bar{X} = \begin{bmatrix} \bar{D}_1 \\ \bar{N}_1 \\ \bar{A}_1 \\ \bar{D}_2 \\ \bar{N}_2 \\ \bar{A}_2 \end{bmatrix}, \quad \text{and} \quad \begin{cases} F_1(X) = \frac{\lambda^\alpha}{1+\theta^\alpha A_1} - f^\alpha D_1 N_2 - d^\alpha D_1, \\ F_2(X) = \lambda_N^\alpha + f^\alpha D_2 N_1 - d^\alpha N_1, \\ F_3(X) = \frac{a^\alpha D_2 N_1}{b^\alpha + D_2 N_1} - d^\alpha A_1, \\ F_4(X) = \frac{\lambda^\alpha}{1+\theta^\alpha A_2} - f^\alpha D_2 N_1 - d^\alpha D_2, \\ F_5(X) = \lambda_N^\alpha + f^\alpha D_1 N_2 - d^\alpha N_2, \\ F_6(X) = \frac{a^\alpha D_1 N_2}{b^\alpha + D_1 N_2} - d^\alpha A_2, \end{cases}$$

then we have

$$\begin{aligned}
&\big\|F(X) - F(\bar{X})\big\| \\
&= \left| \frac{\lambda^\alpha}{1+\theta^\alpha A_1} - \frac{\lambda^\alpha}{1+\theta^\alpha \bar{A}_1} - f^\alpha (D_1 N_2 - \bar{D}_1 \bar{N}_2) - d^\alpha (D_1 - \bar{D}_1) \right| \\
&\quad + \left| f^\alpha (D_2 N_1 - \bar{D}_2 \bar{N}_1) - d^\alpha (N_1 - \bar{N}_1) \right| \\
&\quad + \left| \frac{a^\alpha D_2 N_1}{b^\alpha + D_2 N_1} - \frac{a^\alpha \bar{D}_2 \bar{N}_1}{b^\alpha + \bar{D}_2 \bar{N}_1} - d^\alpha (A_1 - \bar{A}_1) \right| \\
&\quad + \left| \frac{\lambda^\alpha}{1+\theta^\alpha A_2} - \frac{\lambda^\alpha}{1+\theta^\alpha \bar{A}_2} - f^\alpha (D_2 N_1 - \bar{D}_2 \bar{N}_1) - d^\alpha (D_2 - \bar{D}_2) \right| \\
&\quad + \left| f^\alpha (D_1 N_2 - \bar{D}_1 \bar{N}_2) - d^\alpha (N_2 - \bar{N}_2) \right| \\
&\quad + \left| \frac{a^\alpha D_1 N_2}{b^\alpha + D_1 N_2} - \frac{a^\alpha \bar{D}_1 \bar{N}_2}{b^\alpha + \bar{D}_1 \bar{N}_2} - d^\alpha (A_2 - \bar{A}_2) \right| \\
&\leq \left| \frac{\lambda^\alpha}{1+\theta^\alpha A_1} - \frac{\lambda^\alpha}{1+\theta^\alpha \bar{A}_1} \right| + f^\alpha |D_1 N_2 - \bar{D}_1 \bar{N}_2| + d^\alpha |D_1 - \bar{D}_1|
\end{aligned}$$

$$
\begin{aligned}
&+ f^{\alpha}|D_2N_1 - \bar{D}_2\bar{N}_1| + d^{\alpha}|N_1 - \bar{N}_1| + \left|\frac{a^{\alpha}D_2N_1}{b^{\alpha} + D_2N_1} - \frac{a^{\alpha}\bar{D}_2\bar{N}_1}{b^{\alpha} + \bar{D}_2\bar{N}_1}\right| \\
&+ d^{\alpha}|A_1 - \bar{A}_1| + \left|\frac{\lambda^{\alpha}}{1 + \theta^{\alpha}A_2} - \frac{\lambda^{\alpha}}{1 + \theta^{\alpha}\bar{A}_2}\right| + f^{\alpha}|D_2N_1 - \bar{D}_2\bar{N}_1| + d^{\alpha}|D_2 - \bar{D}_2| \\
&+ f^{\alpha}|D_1N_2 - \bar{D}_1\bar{N}_2| + d^{\alpha}|N_2 - \bar{N}_2| + \left|\frac{a^{\alpha}D_1N_2}{b^{\alpha} + D_1N_2} - \frac{a^{\alpha}\bar{D}_1\bar{N}_2}{b^{\alpha} + \bar{D}_1\bar{N}_2}\right| + d^{\alpha}|A_2 - \bar{A}_2| \\
\leq{}& \frac{\lambda^{\alpha}\theta^{\alpha}}{(1 + \theta^{\alpha}A_1)(1 + \theta^{\alpha}\bar{A}_1)}|A_1 - \bar{A}_1| + Mf^{\alpha}|D_1 - \bar{D}_1| + Mf^{\alpha}|N_1 - \bar{N}_1| + d^{\alpha}|D_1 - \bar{D}_1| \\
&+ Mf^{\alpha}|N_1 - \bar{N}_1| + Mf^{\alpha}|D_2 - \bar{D}_2| + d^{\alpha}|N_1 - \bar{N}_1| + a^{\alpha}b^{\alpha}\left|\frac{D_2N_1 - \bar{D}_2\bar{N}_1}{(b^{\alpha} + D_2N_1)(b^{\alpha} + \bar{D}_2\bar{N}_1)}\right| \\
&+ d^{\alpha}|A_1 - \bar{A}_1| + \frac{\lambda^{\alpha}\theta^{\alpha}}{(1 + \theta^{\alpha}A_2)(1 + \theta^{\alpha}\bar{A}_2)}|A_2 - \bar{A}_2| + Mf^{\alpha}|D_2 - \bar{D}_2| + Mf^{\alpha}|N_2 - \bar{N}_2| \\
&+ d^{\alpha}|D_2 - \bar{D}_2| + Mf^{\alpha}|N_2 - \bar{N}_2| + Mf^{\alpha}|D_1 - \bar{D}_1| + d^{\alpha}|N_2 - \bar{N}_2| \\
&+ a^{\alpha}b^{\alpha}\left|\frac{D_1N_2 - \bar{D}_1\bar{N}_2}{(b^{\alpha} + D_1N_2)(b^{\alpha} + \bar{D}_1\bar{N}_2)}\right| + d^{\alpha}|A_2 - \bar{A}_2| \\
\leq{}& Mf^{\alpha}|D_1 - \bar{D}_1| + Mf^{\alpha}|D_1 - \bar{D}_1| + a^{\alpha}b^{\alpha}M|D_1 - \bar{D}_1| + d^{\alpha}|D_1 - \bar{D}_1| \\
&+ Mf^{\alpha}|N_1 - \bar{N}_1| + Mf^{\alpha}|N_1 - \bar{N}_1| + d^{\alpha}|N_1 - \bar{N}_1| + a^{\alpha}b^{\alpha}M|N_1 - \bar{N}_1| \\
&+ \lambda^{\alpha}\theta^{\alpha}|A_1 - \bar{A}_1| + d^{\alpha}|A_1 - \bar{A}_1| \\
&+ Mf^{\alpha}|D_2 - \bar{D}_2| + Mf^{\alpha}|D_2 - \bar{D}_2| + a^{\alpha}b^{\alpha}M|D_2 - \bar{D}_2| + d^{\alpha}|D_2 - \bar{D}_2| \\
&+ Mf^{\alpha}|N_2 - \bar{N}_2| + Mf^{\alpha}|N_2 - \bar{N}_2| + d^{\alpha}|N_2 - \bar{N}_2| + a^{\alpha}b^{\alpha}M|N_2 - \bar{N}_2| \\
&+ \lambda^{\alpha}\theta^{\alpha}|A_2 - \bar{A}_2| + d^{\alpha}|A_2 - \bar{A}_2| \\
={}& \left(2Mf^{\alpha} + a^{\alpha}b^{\alpha}M + d^{\alpha}\right)|D_1 - \bar{D}_1| + \left(2Mf^{\alpha} + a^{\alpha}b^{\alpha}M + d^{\alpha}\right)|N_1 - \bar{N}_1| \\
&+ \left(\lambda^{\alpha}\theta^{\alpha} + d^{\alpha}\right)|A_1 - \bar{A}_1| \\
&+ \left(2Mf^{\alpha} + a^{\alpha}b^{\alpha}M + d^{\alpha}\right)|D_2 - \bar{D}_2| + \left(2Mf^{\alpha} + a^{\alpha}b^{\alpha}M + d^{\alpha}\right)|N_2 - \bar{N}_2| \\
&+ \left(\lambda^{\alpha}\theta^{\alpha} + d^{\alpha}\right)|A_2 - \bar{A}_2| \\
\leq{}& L\|X - \bar{X}\|,
\end{aligned}
$$

where $L = \max\{2Mf^{\alpha} + a^{\alpha}b^{\alpha}M + d^{\alpha}, \lambda^{\alpha}\theta^{\alpha} + d^{\alpha}\}$.

Therefore, the existence and uniqueness are proved.

4 Equilibriums and stability analysis

In what follows, the equilibriums, stability analysis, and simulations for the two cell model are studied.

4.1 Equilibriums

In this part, the dynamic characteristic of two cells is explored and two scenarios (one is the expression level of Delta is 0, another is not) are considered.

When the expression level of Delta is 0, namely $\lambda = 0$, the equilibrium is

$$
D_1^0 = D_2^0 = 0, \qquad N_1^0 = N_2^0 = \frac{\lambda_N^{\alpha}}{d^{\alpha}}, \qquad A_1^0 = A_2^0 = 0, \qquad E_0 = \left(0, \frac{\lambda_N^{\alpha}}{d^{\alpha}}, 0, 0, \frac{\lambda_N^{\alpha}}{d^{\alpha}}, 0\right).
$$

When the expression of Delta is normal or over-expression, the equilibrium is

$$E_1 = \left(D_1^1, N_1^1, A_1^1, D_2^1, N_2^1, A_2^1\right), \quad \text{and} \quad D_1^1 = D_2^1 = \frac{d^\alpha N_1^1 - \lambda_N^\alpha}{d^\alpha N_1^1},$$

$$A_1^1 = A_2^1 = \frac{a^\alpha (d^\alpha N_1^1 - \lambda_N^\alpha)}{d^\alpha [b^\alpha d^\alpha + (d^\alpha N_1^1 - \lambda_N^\alpha)]},$$

where $N_1^1 = N_2^1$ is the solution of equation (6):

$$\begin{aligned} &d^\alpha f^\alpha N^2 + \left(d^{2\alpha} + \lambda_N^\alpha f^\alpha\right) N - d^\alpha \lambda_N^\alpha \\ &\quad = \frac{\lambda^\alpha d^{2\alpha} f^\alpha N^2 + \lambda^\alpha d^\alpha f^\alpha (b^\alpha f^\alpha - \lambda_N^\alpha) N}{(d^{2\alpha} + a^\alpha \theta^\alpha d^\alpha) N + (d^\alpha b^\alpha f^\alpha - d^\alpha \lambda_N^\alpha - a^\alpha \theta^\alpha \lambda_N^\alpha)}. \end{aligned} \tag{6}$$

Simplify equation (6) and get the following form:

$$\begin{aligned} &d^\alpha f^\alpha \left(d^{2\alpha} + a^\alpha \theta^\alpha d^\alpha\right) N^3 + \left[\left(d^{2\alpha} + a^\alpha \theta^\alpha d^\alpha\right)\left(d^{2\alpha} + \lambda_N^\alpha f^\alpha\right)\right. \\ &\quad + d^\alpha f^\alpha \left(d^\alpha b^\alpha f^\alpha - d^\alpha \lambda_N^\alpha - a^\alpha \theta^\alpha \lambda_N^\alpha\right) - \lambda^\alpha d^{2\alpha} f^\alpha \Big] N^2 \\ &\quad + \left[\left(d^{2\alpha} + \lambda_N^\alpha f^\alpha\right)\left(d^\alpha b^\alpha f^\alpha - d^\alpha \lambda_N^\alpha - a^\alpha \theta^\alpha \lambda_N^\alpha\right) - d^\alpha \lambda_N^\alpha \left(d^{2\alpha} + a^\alpha \theta^\alpha d^\alpha\right)\right. \\ &\quad \left. - \lambda^\alpha d^\alpha f^\alpha \left(b^\alpha f^\alpha - \lambda_N^\alpha\right)\right] N - d^\alpha \lambda_N^\alpha \left(d^\alpha b^\alpha f^\alpha - d^\alpha \lambda_N^\alpha - a^\alpha \theta^\alpha \lambda_N^\alpha\right) = 0. \end{aligned} \tag{7}$$

Define

$$\begin{aligned} B_1 &= d^\alpha f^\alpha \left(d^{2\alpha} + a^\alpha \theta^\alpha d^\alpha\right), \\ B_2 &= \left(d^{2\alpha} + a^\alpha \theta^\alpha d^\alpha\right)\left(d^{2\alpha} + \lambda_N^\alpha f^\alpha\right) + d^\alpha f^\alpha \left(d^\alpha b^\alpha f^\alpha - d^\alpha \lambda_N^\alpha - a^\alpha \theta^\alpha \lambda_N^\alpha\right) \\ &\quad - \lambda^\alpha d^{2\alpha} f^\alpha, \\ B_3 &= \left(d^{2\alpha} + \lambda_N^\alpha f^\alpha\right)\left(d^\alpha b^\alpha f^\alpha - d^\alpha \lambda_N^\alpha - a^\alpha \theta^\alpha \lambda_N^\alpha\right) - d^\alpha \lambda_N^\alpha \left(d^{2\alpha} + a^\alpha \theta^\alpha d^\alpha\right) \\ &\quad - \lambda^\alpha d^\alpha f^\alpha \left(b^\alpha f^\alpha - \lambda_N^\alpha\right), \\ B_4 &= -d^\alpha \lambda_N^\alpha \left(d^\alpha b^\alpha f^\alpha - d^\alpha \lambda_N^\alpha - a^\alpha \theta^\alpha \lambda_N^\alpha\right). \end{aligned} \tag{8}$$

Then the equation becomes

$$B_1 N_1^3 + B_2 N_1^2 + B_3 N_1 + B_4 = 0. \tag{9}$$

Calculate equation (9) and get the following solution:

$$N_1 = \sqrt[3]{-\frac{q}{2} + \sqrt{\left(\frac{q}{2}\right)^2 + \left(\frac{p}{3}\right)^3}} + \sqrt[3]{-\frac{q}{2} - \sqrt{\left(\frac{q}{2}\right)^2 + \left(\frac{p}{3}\right)^3}} - \frac{B_2}{3B_1}, \tag{10}$$

where $p = \frac{3B_1 B_3 - B_2^2}{3B_1^2}$, $q = \frac{27B_1^2 B_4 - 9B_1 B_2 B_3 + 2B_2^3}{27B_1^3}$.

4.2 Stability analysis

In this subsection, the stability of E_0 and E_1 is explored [21–24]. Firstly, we compute the Jacobi matrix as follows:

$$Jac = \begin{bmatrix} -f^\alpha N - d^\alpha & -f^\alpha D & -\frac{\theta^\alpha \lambda^\alpha}{(1+\theta^\alpha A)^2} \\ f^\alpha N & f^\alpha D - d^\alpha & 0 \\ \frac{a^\alpha b^\alpha N}{(b^\alpha + DN)^2} & \frac{a^\alpha b^\alpha D}{(b^\alpha + DN)^2} & -d^\alpha \end{bmatrix}. \tag{11}$$

Then, we get the characteristic determinant

$$\left|S^\alpha I - Jac\right| = \begin{vmatrix} S^\alpha + f^\alpha N + d^\alpha & f^\alpha D & \frac{\theta^\alpha \lambda^\alpha}{(1+\theta A)^2} \\ -f^\alpha N & S^\alpha - f^\alpha D + d^\alpha & 0 \\ -\frac{a^\alpha b^\alpha N}{(b^\alpha + DN)^2} & -\frac{a^\alpha b^\alpha D}{(b^\alpha + DN)^2} & S^\alpha + d^\alpha \end{vmatrix}. \tag{12}$$

Let $\xi = S^\alpha$ and when there is no expression of Delta ($\lambda = 0$), the characteristic determinant becomes

$$\left(\xi + d^\alpha\right)\left(\xi + d^\alpha\right)\left[\xi + \frac{\lambda_N^\alpha f^\alpha}{d^\alpha} + d^\alpha\right] = 0 \tag{13}$$

and the corresponding eigenvalues are $\xi_{1,2} = -d^\alpha$, $\xi_3 = -\frac{\lambda_N^\alpha f^\alpha}{d^\alpha} - d^\alpha$. Obviously, $|\arg(S_{1,2,3})| > \frac{\alpha\pi}{2}$. Therefore, when $\lambda = 0$, the equilibrium $E_0 = (0, \frac{\lambda_N^\alpha}{d^\alpha}, 0, 0, \frac{\lambda_N^\alpha}{d^\alpha}, 0)$ is locally asymptotically stable [21].

In order to verify the validity of the theoretical analysis results, the numerical simulations have been done. According to our previous work [18], the parameters are shown in Table 1, and the time span is [0, 4000]. The initial values are 0.5, 0.5, 0.5, 0.5, 0.5, 0.5, respectively.

Based on the parameters in Table 1, we have calculated the equilibrium $E_0 = (0, 6.0165, 0, 0, 6.0165, 0)$ and the dynamical trends of Delta, Notch, and active Notch are shown when $\lambda = 0$ (Fig. 3). The blue line represents the concentration of Delta, the red line represents the concentration of Notch, and the green line represents the concentration of active Notch. Besides, by changing the order (α) of fractional differential equations from 0.9 to 0.99, the trends are the same, but the equilibrium is bigger with the increase of the order.

The numerical solution of system (5) has the following form:

$$\begin{cases} D_1(t_k) = [\frac{\lambda^\alpha}{1+\theta^\alpha A_1(t_{k-1})} - f^\alpha D_1(t_{k-1})N_2(t_{k-1}) - d^\alpha D_1(t_{k-1})]h^{q_1} - \sum_{j=\nu}^{k} c_j^{(q_1)} D_1(t_{k-j}), \\ N_1(t_k) = [\lambda_N^\alpha + f^\alpha D_2(t_{k-1})N_1(t_{k-1}) - d^\alpha N_1(t_{k-1})]h^{q_1} - \sum_{j=\nu}^{k} c_j^{(q_1)} N_1(t_{k-j}), \\ A_1(t_k) = [\frac{a^\alpha D_2(t_{k-1})N_1(t_{k-1})}{b^\alpha + D_2(t_{k-1})N_1(t_{k-1})} - d^\alpha A_1(t_{k-1})]h^{q_1} - \sum_{j=\nu}^{k} c_j^{(q_1)} A_1(t_{k-j}), \\ D_2(t_k) = [\frac{\lambda^\alpha}{1+\theta^\alpha A_2(t_{k-1})} - f^\alpha D_2(t_{k-1})N_1(t_{k-1}) - d^\alpha D_2(t_{k-1})]h^{q_1} - \sum_{j=\nu}^{k} c_j^{(q_1)} D_2(t_{k-j}), \\ N_2(t_k) = [\lambda_N^\alpha + f^\alpha D_1(t_{k-1})N_2(t_{k-1}) - d^\alpha N_2(t_{k-1})]h^{q_1} - \sum_{j=\nu}^{k} c_j^{(q_1)} N_2(t_{k-j}), \\ A_2(t_k) = [\frac{a^\alpha D_1(t_{k-1})N_2(t_{k-1})}{b^\alpha + D_1(t_{k-1})N_2(t_{k-1})} - d^\alpha A_2(t_{k-1})]h^{q_1} - \sum_{j=\nu}^{k} c_j^{(q_1)} A_2(t_{k-j}), \end{cases}$$

Table 1 The parameters for simulation

Parameter	λ	f	d	λ_N	a	b	θ	α
Value	0/1000	0.01	0.01	0.07	0.01	200	1e6	0.9

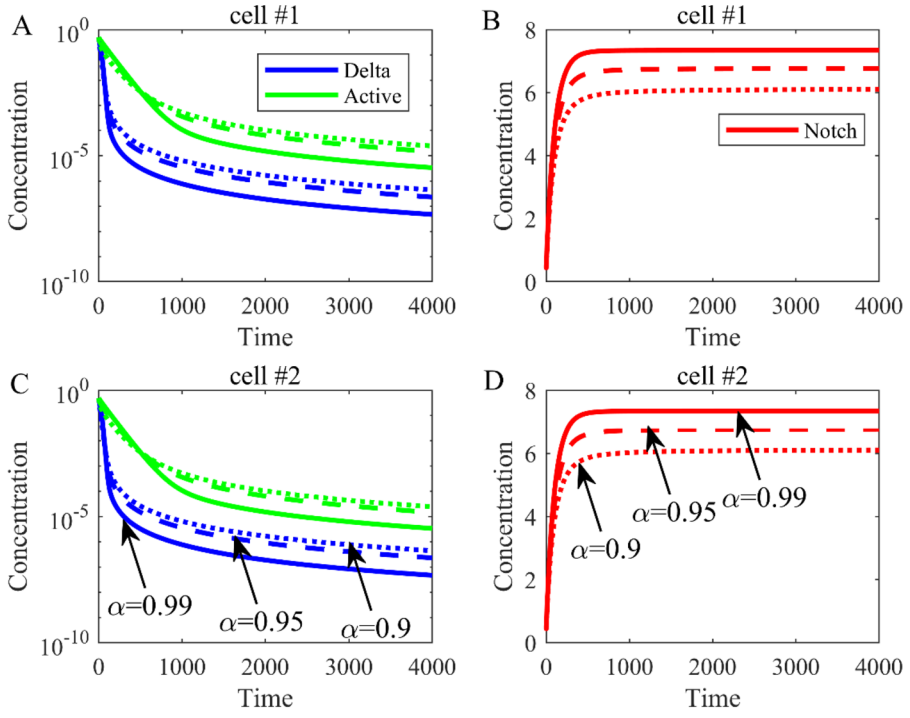

Figure 3 The dynamical trend of Delta, Notch, and active Notch when there is no expression of Delta ($\lambda = 0$). (**A**) The dynamical trend of Delta and active Notch in cell 1. (**B**) The dynamical trend of Notch in cell 1. (**C**) The dynamical trend of Delta and active Notch in cell 2. (**D**) The dynamical trend of Notch in cell 2

where T_{sim} is the simulation time, $k = 1, 2, 3, \ldots, N$, for $N = [T_{\mathrm{sim}}/h]$, and $(D_1(0), N_1(0), A_1(0), D_2(0), N_2(0), A_2(0))$ is the initial condition. The binomial coefficients $c_j^{(q_i)}$ for $\forall i$ are calculated according to the relation $c_0^{(q)} = 1$, $c_j^{(q)} = (1 - \frac{1+q}{j})c_{j-1}^{(q)}$.

Next, the local asymptotic stability at $E_1 = (D_1^1, N_1^1, A_1^1, D_2^1, N_2^1, A_2^1)$ will be explored.

When $\lambda \neq 0$, the characteristic equation is

$$\begin{aligned}
&\xi^3 + \left(f^\alpha N - f^\alpha D + 3d^\alpha\right)\xi^2 + \left[2d^\alpha f^\alpha N - 2d^\alpha f^\alpha D + 3d^{2\alpha}\right. \\
&\quad \left. + \frac{a^\alpha b^\alpha \theta^\alpha \lambda^\alpha N}{(1+\theta^\alpha A)^2 (b^\alpha + DN)^2}\right]\xi + \left[-d^{2\alpha} f^\alpha D + d^{2\alpha} f^\alpha N + d^{3\alpha}\right. \\
&\quad \left. + \frac{a^\alpha b^\alpha \theta^\alpha \lambda^\alpha d^\alpha N}{(1+\theta^\alpha A)^2 (b^\alpha + DN)^2}\right] = 0. \qquad (14)
\end{aligned}$$

Define

$$\begin{aligned}
a_3 &= 1, \\
a_2 &= f^\alpha N - f^\alpha D + 3d^\alpha, \\
a_1 &= 2d^\alpha f^\alpha N - 2d^\alpha f^\alpha D + 3d^{2\alpha} + \frac{a^\alpha b^\alpha \theta^\alpha \lambda^\alpha N}{(1+\theta^\alpha A)^2 (b^\alpha + DN)^2}, \\
a_0 &= -d^{2\alpha} f^\alpha D + d^{2\alpha} f^\alpha N + d^{3\alpha} + \frac{a^\alpha b^\alpha \theta^\alpha \lambda^\alpha d^\alpha N}{(1+\theta^\alpha A)^2 (b^\alpha + DN)^2}.
\end{aligned}$$

According to the Routh–Hurwitz criterion [21], the stable conditions are $a_3 > 0$, $a_2 > 0$, $a_1 > 0$, $a_0 > 0$, and $a_2a_1 - a_3a_0 > 0$.

Proof $a_3 = 1 > 0$ is obviously true.

$$\begin{aligned} a_2 &= f^\alpha N - f^\alpha D + 3d^\alpha \\ &= f^\alpha N - \frac{f^\alpha d^\alpha N - f^\alpha \lambda_N}{d^\alpha N} + 3d^\alpha = \frac{f^\alpha d^\alpha N^2 + (3d^{2\alpha} - f^\alpha d^\alpha)N + f^\alpha \lambda_N}{d^\alpha N}. \end{aligned}$$

If $(3d^{2\alpha} - f^\alpha d^\alpha)^2 - 4f^{2\alpha} d^\alpha \lambda_N^\alpha < 0$, namely $\frac{9d^{3\alpha} + f^{2\alpha} d^\alpha}{4f^{2\alpha}\lambda_N^\alpha + 6f^\alpha d^{2\alpha}} < 1$, we have $a_2 > 0$. When $\frac{d^{3\alpha} + f^{2\alpha} d^\alpha}{4f^{2\alpha}\lambda_N^\alpha + 2f^\alpha d^{2\alpha}} < 1$, $a_3 > 0$, $a_2 > 0$, $a_1 > 0$, $a_0 > 0$.

$$\begin{aligned} &a_2a_1 - a_3a_0 \\ &= \left(f^\alpha N - f^\alpha D + 3d^\alpha\right) \times \left[2d^\alpha f^\alpha (N - D) + 3d^{2\alpha} + \frac{a^\alpha b^\alpha \theta^\alpha \lambda^\alpha N}{(1 + \theta^\alpha A)^2 (b^\alpha + DN)^2}\right] \\ &\quad + d^{2\alpha} f^\alpha D - d^{2\alpha} f^\alpha N - d^{3\alpha} - \frac{a^\alpha b^\alpha \theta^\alpha \lambda^\alpha d^\alpha N}{(1 + \theta^\alpha A)^2 (b^\alpha + DN)^2} > 0 \\ &= 2d^\alpha f^{2\alpha} N^2 - 2d^\alpha f^{2\alpha} DN + 3d^{2\alpha} fN + \frac{a^\alpha b^\alpha \theta^\alpha \lambda^\alpha f^\alpha N^2}{(1 + \theta^\alpha A)^2 (b^\alpha + DN)^2} - 2d^\alpha f^{2\alpha} DN \\ &\quad + 2d^\alpha f^{2\alpha} D^2 - 3d^{2\alpha} f^\alpha D - \frac{a^\alpha b^\alpha \theta^\alpha \lambda^\alpha f^\alpha DN}{(1 + \theta^\alpha A)^2 (b^\alpha + DN)^2} + 6d^{2\alpha} f^\alpha N - 6d^{2\alpha} f^\alpha D + 9d^{3\alpha} \\ &\quad + \frac{3a^\alpha b^\alpha \theta^\alpha \lambda^\alpha d^\alpha N}{(1 + \theta^\alpha A)^2 (b^\alpha + DN)^2} + d^{2\alpha} f^\alpha D - d^{2\alpha} f^\alpha N - d^{3\alpha} - \frac{a^\alpha b^\alpha \theta^\alpha \lambda^\alpha d^\alpha N}{(1 + \theta^\alpha A)^2 (b^\alpha + DN)^2} > 0 \\ &= 2d^\alpha f^{2\alpha} N^2 + 8d^{2\alpha} f^\alpha N - 4d^\alpha f^{2\alpha} DN + 2d^\alpha f^{2\alpha} D^2 - 8d^\alpha f^{2\alpha} D + 8d^{3\alpha} \\ &\quad + \frac{a^\alpha b^\alpha \theta^\alpha \lambda^\alpha (f^\alpha N^2 - f^\alpha DN + 2d^\alpha N)}{(1 + \theta^\alpha A)^2 (b^\alpha + DN)^2} > 0 \\ &= 2d^\alpha \left[f^{2\alpha} (N - D)^2 + 4d^\alpha f^\alpha (N - D) + 4d^{2\alpha}\right] + \frac{a^\alpha b^\alpha \theta^\alpha \lambda^\alpha (f^\alpha N^2 + d^\alpha N + \lambda_N^\alpha)}{(1 + \theta^\alpha A)^2 (b^\alpha + DN)^2} \\ &= 2d^\alpha \left[f^\alpha (N - D) + 2d^\alpha\right]^2 + \frac{a^\alpha b^\alpha \theta^\alpha \lambda^\alpha (f^\alpha N^2 + d^\alpha N + \lambda_N^\alpha)}{(1 + \theta^\alpha A)^2 (b^\alpha + DN)^2} > 0. \end{aligned}$$

Therefore, $a_2a_1 - a_3a_0 > 0$. Using the Routh–Hurwitz criterion [21], when $\frac{d^{3\alpha} + f^{2\alpha} d^\alpha}{4f^{2\alpha}\lambda_N^\alpha + 2f^\alpha d^{2\alpha}} < 1$, $|\arg(S_{1,2,3})| > \frac{\alpha\pi}{2}$, equilibrium $E_1 = (D_1, N_1, A_1, D_2, N_2, A_2)$ is locally asymptotically stable.

All the parameters and initial values are the same except $\lambda = 1000$. The equilibrium is $E_1 = (0.2349, 6.1065, 0.0405, 0.2349, 6.1065, 0.0405)$ and the simulation results are shown in Fig. 4. Similarly, when the order (α) of fractional differential equations varies from 0.9 to 0.99, the trends are the same, and the equilibrium is bigger with the increase of order. This suggests that the order of fractional differential equation can affect the equilibrium. □

5 Sensitivity analysis

Sensitivity analysis is a method to identify critical inputs (parameters) of a model and quantify how input uncertainty impacts model outcome [25]. We conduct sensitivity anal-

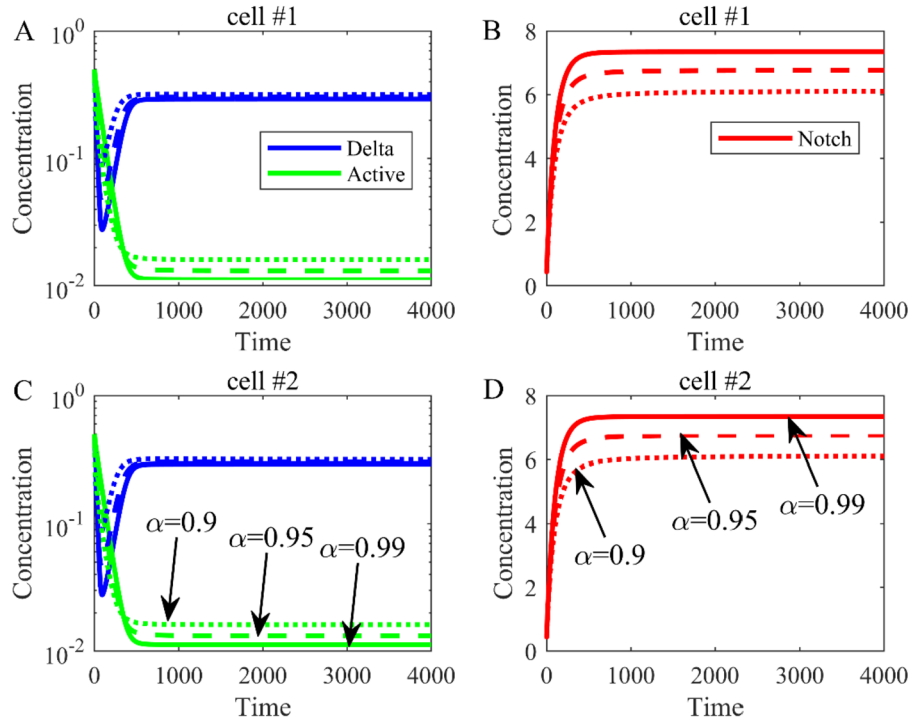

Figure 4 The dynamical trend of Delta, Notch, and active Notch when $\lambda \neq 0$. (**A**) The dynamical trend of Delta and active Notch in cell 1. (**B**) The dynamical trend of Notch in cell 1. (**C**) The dynamical trend of Delta and active Notch in cell 2. (**D**) The dynamical trend of Notch in cell 2

Table 2 The sensitivity values of eight parameters

Parameters	λ	f	d	λ_N	a	b	α	θ
S_i	5.27e−05	2.233	18.933	1.941	1.424	2.263	2.864	2.32e−07

ysis to investigate the significance of parameters by the Morris method. The basic idea is to assess the change in the response output caused by a small variation of parameter.

5.1 Sensitivity values of eight parameters in the two cell model

Assume that the base effect of a model can be represented as the following equation:

$$d_i(j) = \frac{f(x_1, x_2, \ldots, x_{i-1}, x_i + \Delta, x_{i+1}, \ldots, x_n) - f(x_1, \ldots, x_n)}{\Delta}, \tag{15}$$

where $d_i(j)$ is the base effect of the ith parameter in j group ($j = 1, 2, 3, \ldots, R$). R is the number of repeated sampling. n is the number of parameters. x_i is the ith parameter, and Δ is the small variation of parameter. $f(\bullet)$ is the response output. The sensitivity can be calculated by the following equation:

$$S_i = \frac{1}{R} \sum_{j=1}^{R} \left| d_i(j) \right|. \tag{16}$$

The sensitivity values of eight parameters are shown in Table 2.

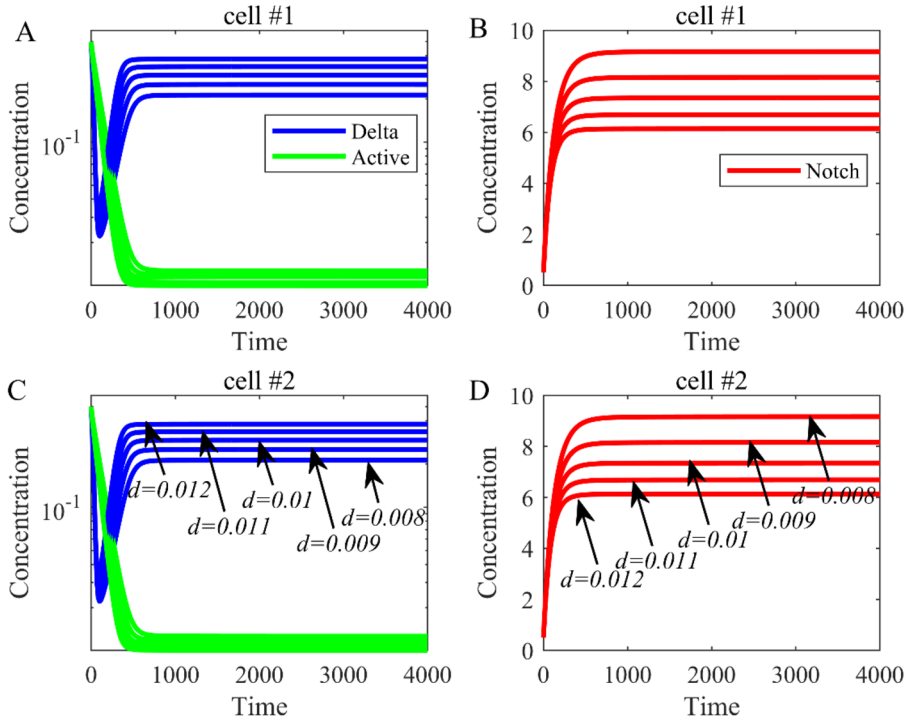

Figure 5 The sensitivity test of d from 0.008 to 0.012. (**A**) The dynamical trend of Delta and active Notch in cell 1. (**B**) The dynamical trend of Notch in cell 1. (**C**) The dynamical trend of Delta and active Notch in cell 2. (**D**) The dynamical trend of Notch in cell 2

5.2 Sensitivity test in the two cell model

In this subsection, we test the sensitivity of parameters by numerical simulation. Firstly, we verify parameters d and λ in the two cell model. Based on Table 1, the parameter d is 0.01, and we change d from 0.008 to 0.012 with a step 0.001. The results as shown in Fig. 5 illustrate that parameter d with small perturbations can have a large effect on the output of Delta ligand (blue line) and Notch receptor (red line) in the two cell model.

Similarly, the parameter λ is 1000 at the beginning, and we change it from 600 to 1400 with a step 200. The results as shown in Fig. 6 suggest that there is no obvious change in Notch receptor (red line) and only a little change in Delta ligand (blue line).

According to the numerical simulations above, the sensitive parameter can significantly affect the expression of Delta ligands and Notch receptors, while the insensitive parameter cannot.

5.3 Sensitivity test in 60 cells

Based on the sensitivity analysis in two cells, a 60 cell model with 180 dimensional fractional-order differential equations has been verified using numerical simulation.

5.3.1 Phenotype changes due to parameter d changes

Firstly, 60 cells were arranged into 5 rows $\times$ 12 columns, and the parameter λ was defined $\lambda = 1000$ in the first three rows, $\lambda = 0$ in the fourth and fifth rows. Other parameters were chosen as in Table 1 except $d = 0.018$. Blue intensity denotes the expression of Notch levels. Then, we get the wild-type phenotype dyed in deep color in the middle row and in

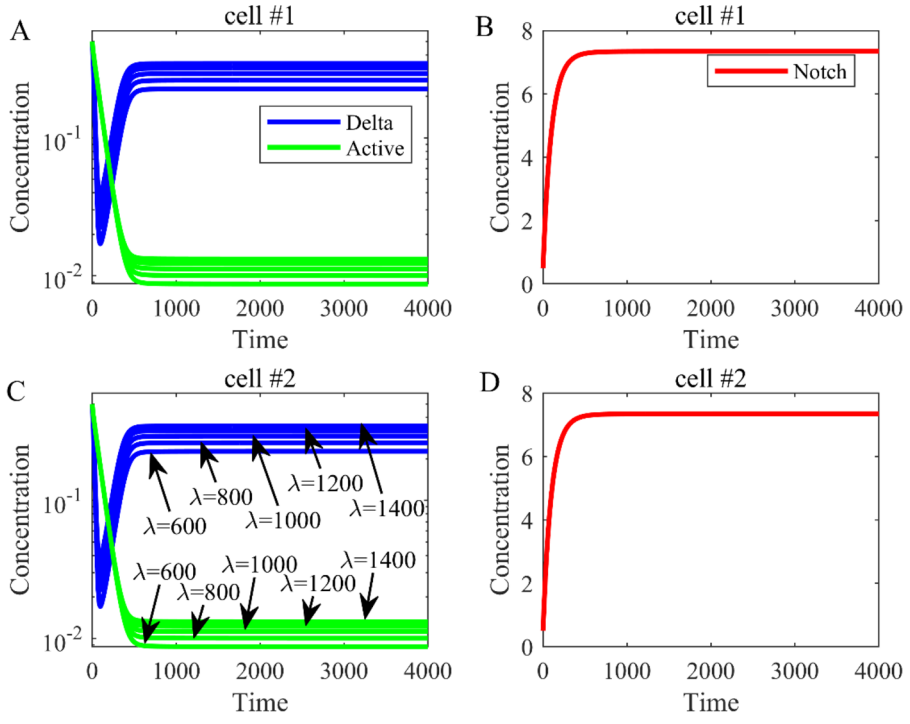

Figure 6 The sensitivity test of λ from 600 to 1400. (**A**) The dynamical trend of Delta and active Notch in cell 1. (**B**) The dynamical trend of Notch in cell 1. (**C**) The dynamical trend of Delta and active Notch in cell 2. (**D**) The dynamical trend of Notch in cell 2

Figure 7 The wild-type phenotype dyed in deep color in the middle row and in light color in others when $d = 0.018$

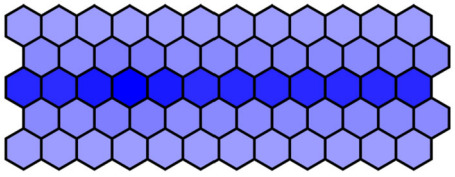

light color in others. The wild-type phenotype obtained from the numerical simulation as shown in Fig. 7 is consistent with the experimental findings (Fig. 1(a)).

Then, we decrease d from 0.018 to 0.001 with a step 0.001 and run simulation to obtain the simulation results. When $d = 0.012$ and other parameters remain unchanged, we get the mutant phenotype the first three rows of which are dyed in deep color and the fourth and fifth rows in light color with over-expressed Notch in the first three rows. The mutant phenotype is shown in Fig. 8 and is consistent with experimental findings (Fig. 1(b)). When $d = 0.001$, the Notch in five rows is all over-expressed, and then five rows are all dyed in deep color. The complete mutant phenotype is shown in Fig. 9 and is consistent with the experimental findings (Fig. 1(c)).

So far, we have obtained the phenotypes of all the current experimental results through numerical simulation by changing sensitive parameter d. This also indirectly shows that the model established in this paper is effective.

Figure 8 The mutant phenotype dyed in deep color in the first three rows and in light color in the fourth and fifth rows when $d = 0.012$

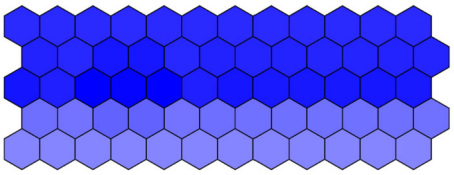

Figure 9 The complete mutant phenotype dyed in deep color in all five rows when $d = 0.001$

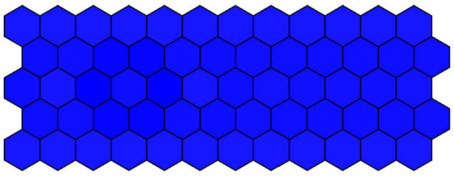

Figure 10 The wild-type phenotype dyed in deep color in the middle row and in light color in others when $\lambda = 1000$

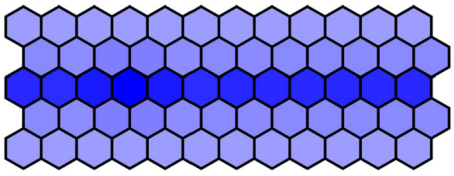

Figure 11 The wild-type phenotype dyed in deep color in the middle row and in light color in others when $\lambda = 1500$

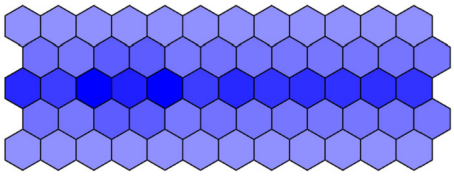

Figure 12 The wild-type phenotype dyed in deep color in the middle row and in light color in others when $\lambda = 2000$

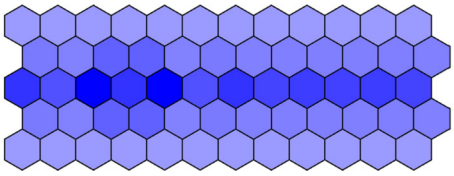

5.3.2 Phenotype changes due to parameter λ changes

In this subsection, we research how phenotype changes due to parameter λ changes. Firstly, fix $d = 0.018$ and gradually increase λ from 1000 to 2000 with a step 200 and then run simulation to obtain the simulation results.

It seems intuitively clear that all phenotypes (Figs. 10–12) are similar because they are all dyed in deep color in the middle row and in light color in others when we increase λ from 1000 to 2000. This also indirectly indicates that the effect of the parameter λ on the phenotype is not significant.

In conclusion, the verification of sensitivity analysis above shows that sensitive parameter d can obviously influence the phenotype, while relatively insensitive parameter λ cannot. This suggests the sensitivity analysis in our model is reliable, and we can minorly adjust the sensitive parameters to obtain ideal phenotypes.

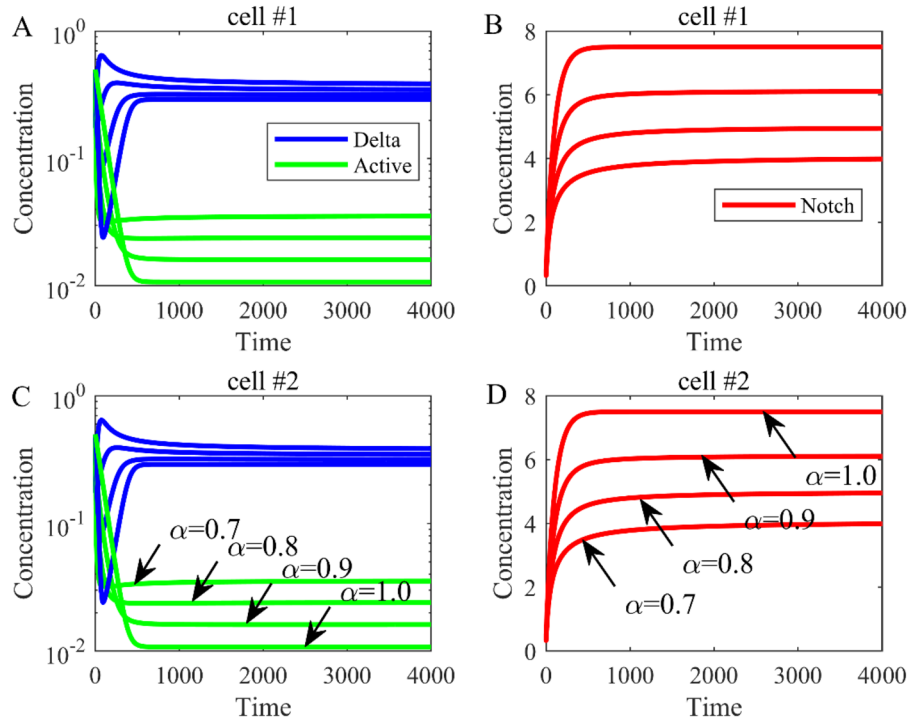

Figure 13 The dynamic between the fractional-order model and the integer-order model in two cells. (**A**) The dynamical trend of Delta and active Notch in cell 1. (**B**) The dynamical trend of Notch in cell 1. (**C**) The dynamical trend of Delta and active Notch in cell 2. (**D**) The dynamical trend of Notch in cell 2

6 Comparison between the fractional-order model and the integer-order model

In this section, the comparison is done between the fractional-order model and the integer-order model in two cells and 60 cells models.

6.1 The comparison in two cells

Firstly, the dynamic between the fractional-order model and the integer-order model in two cells is compared, where the order is $\alpha = 0.9, 0.8, 0.7$ in the fractional-order model and $\alpha = 1$ in the integer-order model (Fig. 13). The simulation results show that under the same parameter value, although both the fractional-order model and the integer-order model reach the equilibrium, the equilibrium point is different. For instance, when $\alpha = 0.9$ the equilibrium of the fractional-order model is $(0.2349, 6.1065, 0.0405, 0.2349, 6.1065, 0.0405)$ and the equilibrium of the integer-order model is $(0.2073, 7.5000, 0.0302, 0.2073, 7.5000, 0.0302)$ when $\alpha = 1$.

6.2 The comparison in 60 cells

In this part, the dynamic between the fractional-order model and the integer-order model in 60 cells is studied to explore how orders affect the phenotype. Similar to the situation of two cells, the dynamic trends of 60 cells are studied firstly. The results show that compared to the integer-order model (the solid line), the equilibrium of the integer-order model (the dotted lines) is obviously smaller (Fig. 14).

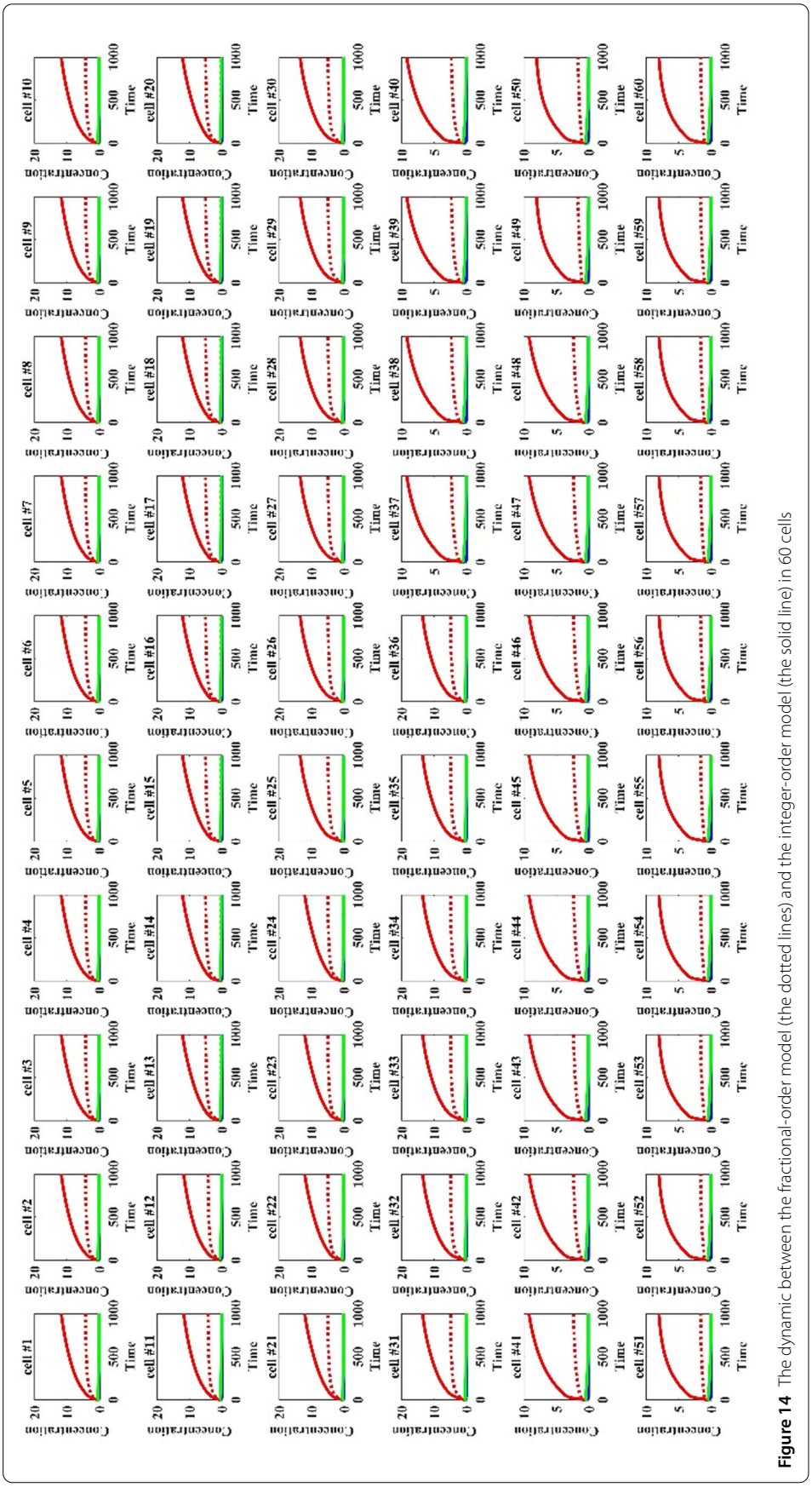

Figure 14 The dynamic between the fractional-order model (the dotted lines) and the integer-order model (the solid line) in 60 cells

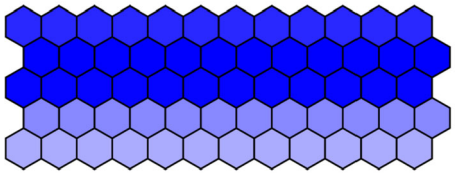

Figure 15 The mutant phenotype dyed in deep color in the first three rows and in light color in the fourth and fifth rows when $\alpha = 0.7$ and $d = 0.004$

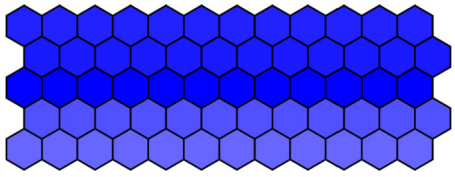

Figure 16 The mutant phenotype dyed in deep color in the first three rows and in medium color in the fourth and fifth rows when $\alpha = 1$ and $d = 0.004$

Next, the phenotypes have been analyzed between the fractional-order model and the integer-order model in 60 cells. In this part, we only studied the effect of parameter d changes on the phenotype, and the method of other parameters is similar. When $\alpha = 0.7$ and $d = 0.004$, the first three rows were dyed in deep color and the fourth and fifth rows were dyed in light color (Fig. 15). If $\alpha = 1$ and $d = 0.004$, the first three rows were dyed in deep color and the fourth and fifth rows were dyed in medium color (Fig. 16). Therefore, it is necessary to study the orders because fractional order can result in different phenotypes.

7 Conclusion

In this paper, an improved mathematical model based on fractional-order differential equations for the Delta-Notch dependent boundary formation in the *Drosophila* large intestine was proposed for the first time. Because Notch signaling pathway is highly conserved in evolution and has significant hereditary properties, fractional differential equation which can better describe the memory characteristics and historical dependence of biological systems was used. We then calculated two equilibriums and studied the local asymptotic stability and also numerically illustrated the stability. Based on numerical simulation in the two cells model, we found that the order of the fractional-order differential equation can significantly affect the equilibrium point.

Moreover, parameter sensitivity analysis showed that different parameters have different sensitivities. The most and least sensitive parameters in the two cells model and the 60 cells model were verified by numerical simulations. The results demonstrated that a small change of sensitive parameter can significantly affect phenotype, while insensitive parameters cannot. Based on our established model, sensitivity analysis can help us to explore key parameters which can obviously affect phenotype, and we can get the ideal phenotype by adjusting these sensitive parameters.

Finally, the comparison was done between the fractional-order model and the integer-order model in two cells and 60 cells models. The results showed that the equilibriums and phenotypes of the fractional-order model are actually different from those of the integer-order model. For example, the expression of Notch is higher than that in the fractional-order model.

In the following, we will do some experiments and estimate an appropriate fractional order by the actual experimental data. What is more, we will compare and evaluate the fitting effects between the fractional-order model and the integer-order model.

Acknowledgements
The authors would like to express their gratitude to the editor and the anonymous referees for their constructive comments and suggestions which have improved the quality of the manuscript.

Funding
This work is supported by the National Natural Science Foundation of China(51675124), (61873094), China Postdoctoral Science Foundation (2020M672829), Shenzhen Peacock Project (KQTD20170331100838136).

Availability of data and materials
No data were used to support this study.

Competing interests
The authors declare that there are no conflicts of interests regarding the publication of this paper.

Authors' contributions
DS built and analyzed the model. LL helped to perform the simulations. FL and JX provided the biological knowledge. LD and DW helped to revise the paper. All authors read and approved the final manuscript.

Author details
[1]Shenzhen Key Laboratory of Tissue Engineering, Shenzhen Laboratory of Digital Orthopedic Engineering, Shenzhen Second People's Hospital, The First Hospital Affiliated to Shenzhen University, Health Science Center, Shenzhen 518035, P.R. China. [2]Shenzhen Institute of Advanced Technology, Chinese Academy of Sciences, Shenzhen 518035, P.R. China. [3]Nanjing Research Institute of Electronic Engineering, Nanjing 210007, P.R. China. [4]School of Software Engineering, South China University of Technology, Building B7, 510006 Guangzhou, P.R. China.

Publisher's Note

Received: 15 January 2020 Accepted: 13 July 2020 Published online: 23 July 2020

References

1. Takashima, S., Yoshimori, H., Yamasaki, N., Matsuno, K., Murakami, R.: Cell-fate choice and boundary formation by combined action of *Notch* and *engrailed* in the *Drosophila* hindgut. Dev. Genes Evol. **212**, 534–541 (2002)
2. Wang, Y., Zhang, X.-S., Chen, L.: Modelling biological systems from molecules to dynamical networks. BMC Syst. Biol. **6**, S1 (2012)
3. Matsuno, H.: In: Pacific Symposium on Biocomputing 2003 (2003)
4. Matsuno, H., et al.: Experimental observations and simulations by Genomic Object Net of Notch signaling in *Drosophila* multicellular systems. Genome Inform. **13**, 453–454 (2002)
5. Morelli, L.G., Uriu, K., Ares, S., Oates, A.C.: Computational approaches to developmental patterning. Science **336**, 187–191 (2012)
6. Rostamy, D., Mottaghi, E.: Forward and backward bifurcation in a fractional-order SIR epidemic model with vaccination. Iran. J. Sci. Technol. Trans. A, Sci. **42**, 663–671 (2018)
7. Vargas-De-León, C.: Volterra-type Lyapunov functions for fractional-order epidemic systems. Commun. Nonlinear Sci. Numer. Simul. **24**, 75–85 (2015)
8. Kai, D.: A fractional calculus based model for the simulation of an outbreak of Dengue fever. Nonlinear Dyn. **71**, 613–619 (2013)
9. González-Parra, G., Arenas, A.J., Chen-Charpentier, B.M.: A fractional order epidemic model for the simulation of outbreaks of influenza A(H1N1). Math. Methods Appl. Sci. **37**, 2218–2226 (2014)
10. Wang, X., Wang, Z., Xia, J.: Stability and bifurcation control of a delayed fractional-order eco-epidemiological model with incommensurate orders. J. Franklin Inst. **356**, 8278–8295 (2019)
11. Almeida, R.: Analysis of a fractional SEIR model with treatment. Appl. Math. Lett. **84**, 56–62 (2018)
12. Mouaouine, A., Boukhouima, A., Hattaf, K., Yousfi, N.: A fractional order SIR epidemic model with nonlinear incidence rate. Adv. Differ. Equ. **2018**, 160 (2018)
13. Gad, I., Novati, P.: The solution of fractional order epidemic model by implicit Adams methods. Appl. Math. Model. **43**, 78–84 (2016)
14. Carvalho, A.R., Pinto, C.M., Baleanu, D.: HIV/HCV coinfection model: a fractional-order perspective for the effect of the HIV viral load. Adv. Differ. Equ. **2018**, 2 (2018)
15. Pinto, C.M.A., Carvalho, A.R.M.: Diabetes mellitus and TB co-existence: clinical implications from a fractional order modelling. Appl. Math. Model. **68**, 219–243 (2018)
16. Lu, Z., Yu, Y., Chen, Y., Ren, G., Xu, C., Wang, S., Yin, Z.: A fractional-order SEIHDR model for COVID-19 with inter-city networked coupling effects (2020). arXiv:2004.12308
17. Hamaguchi, T., et al.: Dorsoventral patterning of the *Drosophila* hindgut is determined by interaction of genes under the control of two independent gene regulatory systems, the dorsal and terminal systems. Mech. Dev. **129**, 236–243 (2012)
18. Liu, F., Sun, D., Murakami, R., Matsuno, H.: Modeling and analysis of the Delta-Notch dependent boundary formation in the *Drosophila* large intestine. BMC Syst. Biol. **11**, 80 (2017)
19. Suryanto, A., Darti, I., Panigoro, H.S., Kilicman, A.: A fractional-order predator–prey model with ratio-dependent functional response and linear harvesting. Mathematics **7**, 1100 (2019)
20. Mondal, S., Lahiri, A., Bairagi, N.: Analysis of a fractional order eco-epidemiological model with prey infection and type 2 functional response. Math. Methods Appl. Sci. **40**, 6776–6789 (2017)

21. Ahmed, E., et al.: On some Routh–Hurwitz conditions for fractional order differential equations and their applications in Lorenz, Rössler, Chua and Chen systems. Phys. Lett. A **358**, 1–4 (2006)
22. Seydel, R.: Practical Bifurcation and Stability Analysis. Springer, Berlin (1994)
23. Lakshmikantham, V., Leela, S., Martynyuk, A.A.: Stability Analysis of Nonlinear Systems. Springer, Berlin (2015)
24. Khanh, N.H., Huy, N.B.: Stability analysis of a computer virus propagation model with antidote in vulnerable system. Acta Math. Sci. **36**, 49–61 (2016)
25. Li, Z.-h., Jin, X.-l., Liu, H.-l., Xu, X.-g., Wang, J.-h.: Global sensitivity analysis of wheat grain yield and quality and the related process variables from the DSSAT-CERES model based on the extended Fourier Amplitude Sensitivity Test method. J. Integr. Agric. **18**, 1547–1561 (2019)